

Borromean ground state of fermions in two dimensions

A. G. Volosniev, D. V. Fedorov, A. S. Jensen, and N. T. Zinner

Department of Physics and Astronomy, Aarhus University, DK-8000 Aarhus C, Denmark

(Dated: October 2, 2018)

The study of quantum mechanical bound states is as old as quantum theory itself. Yet, it took many years to realize that three-body borromean systems that are bound when any two-body subsystem is unbound are abundant in nature. Here we demonstrate the existence of borromean systems of spin-polarized (spinless) identical fermions in two spatial dimensions. The ground state with zero orbital (planar) angular momentum exists in a borromean window between critical two- and three-body strengths. The doubly degenerate first excited states of angular momentum one appears only very close to the two-body threshold. They are the lowest in a possible sequence of so-called super-Efimov states. While the observation of the super-Efimov scaling could be very difficult, the borromean ground state should be observable in cold atomic gases and could be the basis for producing a quantum gas of three-body states in two dimensions.

PACS numbers:

Unlike classical mechanics quantum mechanics allows bound N -body states without having bound subsystems. These so-called borromean systems are discussed in a number of publications for the simplest example of three particles [1–7]. The phenomenon was recently even generalized to more particles and higher orders, see f.ex. Ref. [8]. Borromean three-body systems are abundant in three dimensions (3D) for both bosonic and fermionic systems in nuclear, atomic and molecular physics [9, 10]. However, the behavior is strikingly different for bosonic systems in one or two (2D) spatial dimensions [11–13], where bound states appear for infinitesimally small attractions. Without an artificial repulsive barrier at large distance it is virtually impossible to form a borromean bosonic 2D system [11–13]. Furthermore, the celebrated Efimov effect of infinitely many bound three-body states at the two-body threshold is not present in 2D [14, 15].

Three identical spin-polarized fermions are harder to bind than bosons, because relative two-body s -states are forbidden by the Pauli principle. It would therefore intuitively be more difficult to form borromean systems and the Efimov effect should be out of reach. However, both effects are possible in 2D as we shall discuss in the present paper. The Efimov effect was recently derived in an extreme double-exponential scaling form [16] using a momentum space formalism. The same scaling behavior was also found in low-energy scattering of three spinless fermions [17].

In this paper we present analytical and numerical evidence for a new state of fermionic matter where the basic constituent is a borromean three-fermion cluster. This may be considered a trion quantum gas as opposed to the two-component BCS-BEC crossover [19, 20] driven by the absence (BCS) or presence (BEC) of a two-body bound state. The new structure should be accessible through the tunability of both interactions and geometry of modern cold atom experiments [10]. Both the single particles and the three-body borromean states are fermionic entities and thus have to obey the Pauli principle. This could imply an increase in stability of the many-body system,

but estimates of the lifetime show that it is expected to be considerably shorter than the two-component Fermi gas [17, 21]. The creation of a superfluid state of spin-polarized fermions is still an important outstanding goal in the field. Observation of the three-body borromean ground state is, however, not dependent on reaching the superfluid state. When formed, these three-body states are likely susceptible to chemical reactions and may be used to study quantum chemical dynamics of a fermionic gas with suppressed two-body but enhanced three-body reactions.

I. TWO FERMIONS AT THE TWO-BODY THRESHOLD FOR BINDING

Borromean states are most easily found for potentials that can almost bind a two-body system. The relative motion in two-body systems is described with the wave function given as a product of radial, $\phi_M(r)$, and angular, $\exp(iM\theta)$, parts, where (r, θ) are the polar relative coordinates, and $M = 0, \pm 1, \pm 2, \dots$ is the 2D angular momentum quantum number. The radial Schrödinger equation is

$$\frac{\hbar^2}{m} \left(-\frac{1}{r} \frac{\partial}{\partial r} r \frac{\partial}{\partial r} + \frac{M^2}{r^2} \right) \phi_M = (E_2 - gV) \phi_M, \quad (1)$$

where the bounded potential, $V(r)$, of cylindrical symmetry is assumed to decrease faster than $1/r^{2+\epsilon}$, $\epsilon > 0$, for large r , or in practice treated as zero outside a finite radius R_0 . The two-body energy is E_2 , $g > 0$, is a dimensionless strength parameter, and m is the mass of one particle. The doubly degenerate antisymmetric ground state for spin polarized fermions has $M = \pm 1$, since $M = 0$ describes a symmetric total wave function. Therefore, for two fermions we shall only consider $M = 1$ and omit the related index. The regular zero energy solution, $\phi(r)$, to Eq. (1) obeys [22]

$$\phi(r) = r - \frac{gm}{2\hbar^2} \int_0^r ds \frac{s^2 - r^2}{r} V(s) \phi(s). \quad (2)$$

V	g_2^{cr}	g_3^{cr}/g_2^{cr}	$E_3(g_2^{cr})$	$E_3^*(g_2^{cr})$	$\langle \rho^2 \rangle_{gr}$	$\langle \rho^2 \rangle_{exc}$
$V_1(r)$	6.72	0.72	-1.50	-0.18	1.65	6.0
$V_2(r)$	28.98	0.68	-5.55	-0.47	0.56	1.13
$V_3(r)$	8.63	0.72	-0.439	-0.045	5.9	22.7

TABLE I: Borromean binding energies. Numerically calculated two-body thresholds for binding, three-body properties at the thresholds and estimates for three-body thresholds for binding. Ground and excited states have angular momentum 0 and ± 1 . Lengths and energies are in units of b and $\hbar^2/(mb^2)$, respectively.

The large-distance asymptotic of this $E_2 = 0$ solution is uniquely determined by the length parameter, a , defined such that $\phi(r)$ asymptotically approaches $(r^2 - a^2)/r$ [5], where

$$a^2 = \frac{\frac{gm}{\hbar^2} \int_0^\infty ds s^2 V(s) \phi(s)}{2 + \frac{gm}{\hbar^2} \int_0^\infty ds \phi(s) V(s)}. \quad (3)$$

The critical value, g_2^{cr} , for two-body binding is reached when $a = \infty$ where the zero-energy solution crosses zero at $r \rightarrow \infty$, see Methods. Then g_2^{cr} is defined as the smallest value of g where the denominator in Eq. (3) vanishes. The limit $g \rightarrow 0$ corresponds to $a \rightarrow 0$, since binding of two identical fermions in 2D requires a finite attraction.

A. Numerical results for two fermions

To address weakly bound two-fermion systems we use the stochastic variational method [23–25] to calculate ground state energies for different values of g . To illustrate the generic nature of our findings, we choose three qualitatively different potentials

$$\begin{aligned} V_1(r) &= -\frac{\hbar^2}{mb^2} e^{-r^2/b^2}, \\ V_2(r) &= -\frac{\hbar^2}{mb^2} (e^{-r^2/b^2} - 0.5e^{-0.5r^2/b^2}), \\ V_3(r) &= \frac{\hbar^2}{mb^2} (e^{-r^2/b^2} - 0.8e^{-0.5r^2/b^2}). \end{aligned} \quad (4)$$

The first has a simple attractive pocket, the second has a repulsive barrier outside the attraction, and the third has a repulsive core. The calculated values of g_2^{cr} are given in Tab. I. The two-body bound states with $E_2 \rightarrow 0$ are universal, independent of potential, i.e. the wave function is a modified Bessel function $K_1(|k|r)$ ($k^2 = mE_2/\hbar^2$), corresponding to $V = 0$ with essentially only non-zero probability in the classically forbidden region of zero potential. Using the wave function, K_1 , in all space we find the mean square radius for small k , i.e.

$$\langle r^2 \rangle |k|^2 \ln(|k|b) = -\frac{2}{3} + O\left(\frac{1}{\ln(|k|b)}\right), \quad (5)$$

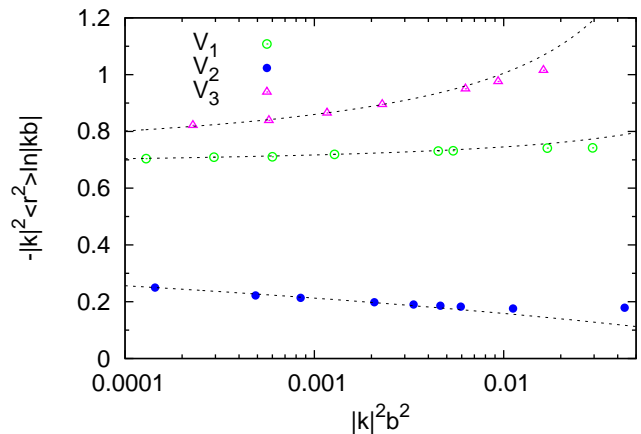


FIG. 1: Asymptotic behaviour of the two-body states. Calculated mean square radii as function of the two-body binding energy for the three potentials in eq. (4). The points are obtained numerically by decreasing the attraction g through the variation $g \rightarrow g_2^{cr}$. The curves are produced by fits with a length parameter, b_0 , in eq. (5) different from b , i.e. we have fitted the numerical results to the functional form on the left-hand side of eq. (5). This incorporates next-to-leading order terms proportional to $[\ln(|k|b)]^{-1}$. The limit for $k = 0$ is $2/3$. The parameters of the fits are $\ln(b_0/b) = 0.4864$ for V_1 , $\ln(b_0/b) = 1.55$ for V_3 and $\ln(b_0/b) = -14.74$ for V_2 .

where we used the potential range parameter, b , to get a dimensionless argument of the logarithm.

To confirm our understanding through Eq. (5) is numerically challenging for some potentials. In Fig. 1 we see that the limit of $2/3$ only is reached for very small E_2 , although much faster for V_1 and V_3 than for V_2 . The different rates of convergence illustrate how small an energy is necessary to reach the universality limit for potentials of varying structure. The similarity for V_1 and V_3 arises because the repulsive core for V_3 is ineffective for the p -waves, while their attractions are similar. On the other hand, the external barrier for V_2 delays tunneling into the universal region of the classically forbidden space and beyond. The radius increases with decreasing k as larger distances are populated. However, the universal limit will eventually be reached for sufficiently small E_2 .

These properties are markedly different for two bosons in 2D where the symmetric wave function with $M = 0$ is well described by $K_0(|k|r)$ at comparably small binding energies [26]. These observations are of crucial importance in understanding the universal two-body bound states that arise near the window for borromean binding.

II. THREE FERMIONS

The two-fermion binding requirement of a finite potential depth in 2D resembles that of two bosons in 3D. This strongly suggests that borromean three-fermion systems

are possible in 2D even for purely attractive potentials. Also, the Efimov effect cannot be strictly ruled out for three spin-polarized fermions in 2D [15]. In contrast, we know that the Efimov effect is absent for three bosons in 2D, and borromean states only occur for potentials with positive net volume, $\int V(r)rdr > 0$, and regions with substantial repulsion [11–15].

In 3D, the coordinate-space adiabatic hyperspherical expansion method proved to be very efficient for short-range interactions due to small large-distance couplings [5]. This efficiency is highlighted in the precise description of the Efimov effect by use of only the lowest adiabatic potential [9, 27, 28]. We shall therefore here employ the 2D hyperspherical formalism [5, 11, 13] for three spin-polarized fermions.

Let \mathbf{r}_i be the coordinate of the i th particle. One set of the relative Jacobi coordinates is $\mathbf{x}_i = (\mathbf{r}_j - \mathbf{r}_k)/\sqrt{2}$ and $\mathbf{y}_i = (\mathbf{r}_j + \mathbf{r}_k)/\sqrt{6} - \sqrt{2/3}\mathbf{r}_i$, while the other sets are obtained by cyclic permutation of $\{i, j, k\} = \{1, 2, 3\}$. The hyperspherical coordinates are given by $\rho = \sqrt{\mathbf{x}_i^2 + \mathbf{y}_i^2}$ and the three angles for each Jacobi set, $\Omega_i = \{\alpha_i, \Theta_{xi}, \Theta_{yi}\}$, where $\alpha_i = \arctan(x_i/y_i)$, and Θ_{xi} and Θ_{yi} define directions of the coordinates $(\mathbf{x}_i, \mathbf{y}_i)$. The kinetic energy operator has the form

$$T = -\frac{\hbar^2}{2m} \left(\rho^{-3/2} \frac{\partial^2}{\partial \rho^2} \rho^{3/2} - \frac{3}{4\rho^2} \right) + \frac{\hbar^2}{2m\rho^2} \Lambda^2 \quad (6)$$

where the hyperangular part is

$$\Lambda^2 = -\frac{\partial^2}{\partial \alpha_i^2} - 2 \cot(2\alpha_i) \frac{\partial}{\partial \alpha_i} - \frac{1}{\sin^2 \alpha_i} \frac{\partial^2}{\partial \Theta_{xi}^2} - \frac{1}{\cos^2 \alpha_i} \frac{\partial^2}{\partial \Theta_{yi}^2}. \quad (7)$$

The eigenfunctions corresponding to the dependence on Θ_{xi} and Θ_{yi} are $\exp(im_{xi}\Theta_{xi} + im_{yi}\Theta_{yi})$, where m_{xi} and m_{yi} are integers. The sum, $M = m_{xi} + m_{yi}$, is a conserved quantum number which labels the solutions by $M = 0, \pm 1, \pm 2, \dots$

The total wave function, Ψ_M , is expanded in a complete set of hyperangular functions, $\Phi_{nM}(\rho, \Omega)$, for each ρ chosen as eigenfunctions of the hyperangular part of the Hamiltonian, $H = T + g \sum_{i=1}^3 V(\sqrt{2}|\mathbf{x}_i|)$. Thus,

$$\Psi_M = \frac{1}{\rho^{3/2}} \sum_{n=0}^{\infty} f_{nM}(\rho) \Phi_{nM}(\rho, \Omega), \quad (8)$$

$$\left(\Lambda^2 + g \frac{2m\rho^2}{\hbar^2} \sum_{i=1}^3 V(\sqrt{2}|\mathbf{x}_i|) \right) \Phi_{nM} = \lambda_{nM}(\rho) \Phi_{nM}, \quad (9)$$

where V is the two-body potential, and the functions $f_{nM}(\rho)$ satisfy a system of coupled equations.

We omit the index n and search only for the angular solution, Φ_M , of lowest energy for a given M . We use the Faddeev decomposition and expansion on the eigenfunctions related to Θ_{xi} and Θ_{yi} , that is

$$\Phi_M = \frac{1}{2\pi} \sum_{m_{xi}, i} \phi_{Mm_{xi}}(\rho, \alpha_i) e^{-im_{xi}\Theta_{xi} - i(M-m_{xi})\Theta_{yi}}, \quad (10)$$

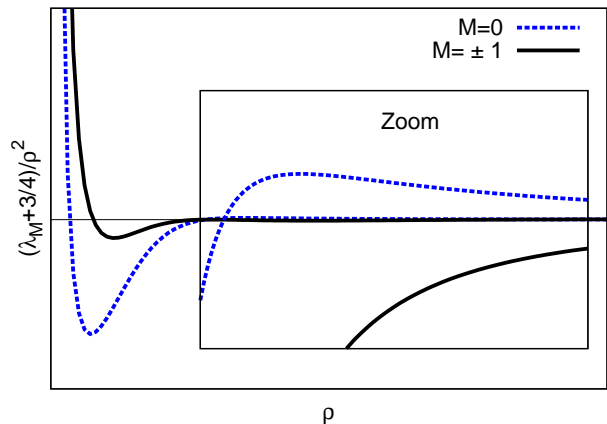


FIG. 2: Three-body potentials for ground state and first excited state channels. Schematic illustration of the lowest adiabatic potentials for $M = 0$ and $M = 1$ at short and long distance. The inset shows a zoom of the behavior at large distance to illustrate the barrier in the $M = 0$ channel. Note that only the vertical axis has been amplified in the inset. The inset starts roughly at the distance $\rho \sim b$. For the potentials considered here the attractive pocket in the $M = 0$ channel is considerably larger than in the $M = 1$ channel. We therefore have stronger binding in the $M = 0$ channel.

where $i = 1, 2, 3$ and the index m_{xi} only assumes odd values to ensure antisymmetry.

A. Lowest order large-distance solution

We first solve to lowest order without any non-adiabatic and coupling terms, that is we find $f_M(\rho)$ in the so-called exact adiabatic approximation [29], from

$$\left(-\frac{\partial^2}{\partial \rho^2} + \frac{\lambda_M + 3/4}{\rho^2} - \frac{2mE_3}{\hbar^2} \right) f_M(\rho) = 0. \quad (11)$$

Using the lowest adiabatic potential produced by λ_M we then get a lower bound on the energy [29]. The behavior of λ_M for large ρ is decisive for sufficiently weakly bound states provided the centrifugal barrier is small.

We find λ_M by solving Eq. (9) with the structure of Φ_M in Eq. (10). In general, the contributing configurations in angular space arise from the smallest $|m_x|$ -values, since the centrifugal barrier in α -space is decided by the $1/(\sin^2 \alpha)$ -term in Eq. (7). For our cases of $M = 0$ and $M = 1$ these values are $(m_x, m_y) = (1, -1), (-1, 1)$ and $(1, 0), (-1, 2)$, respectively. Detailed calculations of λ_M are described in Methods.

With these λ_M we obtain differential equations for $f_M(\rho)$ from Eq. (11), that is

$$\left(-\frac{\partial^2}{\partial \rho^2} + \frac{3}{4\rho^2} - \frac{16}{3\rho^2 \ln(\rho/R_0)} - \frac{2mE_3}{\hbar^2} \right) f_0(\rho) = 0, \quad (12)$$

$$\left(-\frac{\partial^2}{\partial \rho^2} - \frac{1}{4\rho^2} - \frac{16}{9\rho^2 \ln^2(\rho/R_0)} - \frac{2mE_3}{\hbar^2} \right) f_1(\rho) = 0, \quad (13)$$

which are valid for strengths close to g_2^{cr} where $a \rightarrow \infty$.

For $M = 0$, the large-distance behavior is a repulsive centrifugal barrier corresponding to two close-lying particles and the third far away in a state of relative angular momentum 1. This barrier excludes infinitely many bound states. For $M = \pm 1$ the large-distance behavior is attractive with a leading term arising from two particles close to each other and the third far away with relative angular momentum 0. For $E_3 = 0$ an analytical solution can be found as in Ref. [30] and easily proved by insertion into Eq. (13), that is

$$f_1(E_3 = 0, \rho) = \sqrt{\rho \ln \rho} \cos(s \ln(\ln(\rho/R_0)) + \delta), \quad (14)$$

where $s = \sqrt{16/9 - 1/4}$ and the value of δ is related to the short-distance boundary condition. This is an oscillating function of $\ln(\ln(\rho/R_0))$ with an infinite number of nodes. Consequently Eq. (13) has an infinite number of bound state solutions with $E_3 < 0$.

Each of these bound states of energy $E_3^{(n)}$ falls off exponentially when ρ^2 increases above $\rho_n^2 = \hbar^2/(2m|E_3^{(n)}|)$. However, for $\rho < \rho_n$ all solutions resemble $f_1(E_3 = 0, \rho)$, which therefore provides the estimate $-E_3^{(n)} \propto \hbar^2/(2m\rho_n^2)$ where ρ_n obey $s \ln(\ln \rho_n/R_0) + \delta = \pi(n+1/2)$. Thus, $-E_3^{(n)} \sim \exp(-2e^{\pi n/s})$ and we obtain a double exponential scaling. The simultaneous contributions from components, $(m_x, m_y) = (1, 0), (-1, 2)$, are crucial for this conclusion.

B. Higher order effects

The derivation of λ_M from solving the angular equation, Eq. (9), was very recently modified in Ref. [18] by including, in the angular wave function at small angles α , the next order (faster vanishing) term in ρ . Surprisingly, this leads to an additional slower vanishing, non-universal term, $-Y/(\rho^2 \ln(\rho/R_0))$, which should be added in both radial equations Eqs. (12) and (13). For details see Methods.

This unusual behavior suggests that other higher order terms also should be investigated. First, we emphasize that only the angular configurations with $|m_x| \leq 1$ can contribute to a large-distance long-range behavior supporting infinitely many bound states. Second, non-adiabatic coupling terms in the radial equations are expected to vanish faster than the terms included so far. Here the diagonal coupling term [5], $Q = \langle \Phi_1 | \frac{\partial^2}{\partial \rho^2} | \Phi_1 \rangle_{\{\Theta_x, \Theta_y, \alpha\}}$, is of very special significance for two reasons. First, it is expected to be the slowest vanishing for large ρ , and second omission or inclusion of this coupling in the lowest adiabatic potential produces, respectively a lower or upper bound for the exact binding energy [29]. The leading order result for Q is derived in Methods to cancel exactly the non-universal term found in Ref. [18]. As a byproduct $Y > 0$ is simultaneously demonstrated.

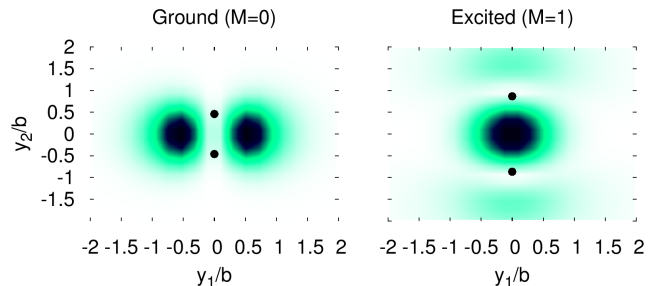


FIG. 3: Three fermion wave functions in ground and excited states. The ground (left) and excited (right) state probability distributions of the third fermion for V_1 at the two-body threshold as function of \mathbf{y} for a fixed value of $\mathbf{x} = (0, \sqrt{\langle x^2 \rangle})$ corresponding to the first two particles fixed at positions $(y_1, y_2) = (0, \pm\sqrt{\langle x^2 \rangle})/2$ indicated by the black dots. The probabilities increase from light (white) to dark (black) colors. The unit of length is b .

Conclusions from these delicate considerations are first that the $M = 0$ channel essentially is unaffected, since this very small additional term cannot change the large-distance main contribution, $3/(4\rho^2)$, of the repulsive centrifugal barrier in Eq. (12). Second, it cannot change the short-distance attraction which is crucial for borromean structures. Third conclusion is that inclusion of these terms are very important for the $M = 1$ channel, since it may change the large-distance behavior crucial for possible (super) Efimov states.

The necessary rigorous mathematical derivations and accurate numerical investigations for $M = 1$ are very involved and beyond the scope of this paper. However, if for instance, the next order of Q is equal to $1/(4\rho^2 \ln^2(\rho/R_0))$ and the sum of all other couplings vanish faster, the prediction in Ref. [16] would be confirmed. We emphasize that this order in Q is crucial for the Efimov effect as it provides both upper and lower bounds on the exact energy.

C. Borromean binding

The ambiguity in the $M = 1$ channel is present but not as important for the $M = 0$ channel, where the short-distance behavior is decisive. The effective potential in Eq. (11) obtained from Eq. (9) is for $\rho = 0$ simply the eigenvalue, $K(K+2)$ of the kinetic energy operator Λ^2 , see Ref. [5]. The Pauli principle selects $K = 2, 3$ for $M = 0, 1$, respectively. The potentials for small ρ are then $35/4\rho^2$ and $63/4\rho^2$. Comparing the potentials at short and large distances we conclude that the effective potentials have to cross each other with more attractions in the $M = 0$ channel at short distances. This behavior is plotted schematically in Fig. 2 which shows that the three-body ground state has $M = 0$.

Let us now consider strengths, g , such that $g_3^{cr} \leq g \leq$

g_2^{cr} , where g_3^{cr} is defined as the limit for binding three fermions. Since the wave function is fully antisymmetric we can use the result in Ref. [3] to obtain a lower bound for the ground state energy, $E_3(m, g) \geq 2E_2(m, 3g/2)$. It then immediately follows that $2/3 \leq g_3^{cr}/g_2^{cr} \leq 1$. As for three bosons in 3D, the lower limit is reached for deep and narrow two-body potentials vanishing at large distance.

To investigate three-body systems numerically we apply the stochastic variational technique to the three-body Schrödinger equation using the basis elements

$$\begin{aligned} \psi_i &= (1 - P_{12})(1 - P_{13})(1 - P_{23})G(\mathbf{x}, \mathbf{y}), \\ G &= e^{-a_1(\mathbf{x}-\mathbf{s}_1)^2 - 2a_2(\mathbf{x}-\mathbf{s}_1)(\mathbf{y}-\mathbf{s}_2) - a_3(\mathbf{y}-\mathbf{s}_2)^2}, \end{aligned} \quad (15)$$

where P_{ij} is the operator that exchanges particle coordinates i and j , and a_k, \mathbf{s}_k are non-linear variational parameters that are found stochastically [23]. In Table I we present the three-body energies, $E_3(g_2^{cr})$, for the ground and doubly degenerate first excited states. Borromean binding is then allowed for strengths smaller than g_2^{cr} with corresponding smaller three-body binding energies. Away from g_2^{cr} the Efimov condition of infinitely large scattering length is violated. The ground state has $M = 0$ for all the qualitatively different two-body potentials, and energies and sizes are of the same order as the potential depths and ranges. The first excited states have much smaller binding energy, much larger extension, and quantum number $M = \pm 1$. They are the first in the possible sequence of super-Efimov states.

The geometric structure of these states can be seen in the probability density, $P = |\Phi(\mathbf{x}, \mathbf{y})|^2$, shown in Fig. 3 for potential V_1 . We choose the \mathbf{x} -coordinate to be $\mathbf{x} = (0, \sqrt{\langle x^2 \rangle})$ with a particle distance equal to the root-mean-square value. The structures in Fig. 3 persist for the other potentials and for different values of $|x|$. The resulting triangular and linear chain structures resemble the ground and the celebrated first excited 0^+ states for the α -cluster structure of the ^{12}C -nucleus [6].

By decreasing g from g_2^{cr} toward g_3^{cr} we move into the borromean window and away from infinite scattering length. This quickly removes all possible $M = \pm 1$ excited bound states. However, the $M = 0$ ground state remains until the value $g = g_3^{cr}$ which is calculated and given in Tab. I. Energies and sizes for $g = g_2^{cr}$ given as mean-square radii, $\langle \rho^2 \rangle$, illustrate both stability and fragility of ground and excited states. Ratios of their binding energies differ consistently with one order of magnitude, and excited state radii are much larger than for the ground state. The effect of the outer barrier in V_2 is clearly seen through larger binding and smaller radii.

III. DISCUSSION

Using a hyperspherical formalism in 2D we have found that three identical fermions support two very different types of bound states corresponding to angular momentum 0 and 1. We find a doubly degenerate excited state

of angular momentum one for two-body potentials very close to the threshold for binding. These states may be the lowest in an infinite sequence of super Efimov states as predicted in Ref. [16]. Our findings differ from Ref. [18] where a non-universal term appears in the effective three-body potential. However, we show that this term is cancelled precisely by inclusion of the leading order of the diagonal coupling. In any case, the possible states are fragile, extremely large and weakly bound, and observation of the related possible super Efimov sequence would be correspondingly difficult.

A novel discovery is the existence of a borromean window defined as an interval in finite two-body strengths where no two-body subsystem is bound. Within this window the well bound zero angular momentum ground state is found to be located inside a barrier. This is in sharp contrast to the system of three bosons [12]. Numerical calculations for three spin-polarized systems are carried out for the first time in two dimensions using the coordinate space formalism with finite-range potentials. The results confirm the analytically discussed properties for both ground and excited states. These calculations can be used as a reference point for further numerical studies, that could be performed with atomic potentials obtained from state-of-the-art quantum chemical calculations.

The ground state Borromean states are located behind an outer barrier as we have demonstrated here. This implies that they should be observable as a peak in the atom loss rate when the state is located in the window for borromean binding precisely as the bosonic Efimov effect has been observed [31–34]. An alternative way to probe and populate the states would be to use RF spectroscopy [35–37]. It is imperative to notice that we do not need the presence of Feshbach resonances in the angular momentum one (p -wave) channel [38]. The method we have used to derive the results above assumes only that there is a short-range two-body potential between the fermions that can be tuned in some way so that one can approach the threshold for the existence of a two-body bound state between two identical fermions. A p -wave Feshbach resonance is one option, but it could also be achieved by using for instance a long-range interaction such as for instance a dipole-dipole force.

Acknowledgements Discussions with D.-W. Wang, J. Levensen, S. Moroz, Y. Nishida and Z. Yu are gratefully acknowledged. This work was funded by the Danish Council for Independent Research DFF Natural Sciences and the DFF Sapere Aude program.

Appendix A: Two-body binding in two dimensions

Here we discuss the behavior of the two-body binding energy near the threshold. At this point we also would like to refer to some early works [39] using Jost function formalism. For our derivations we use [26] that the discrete spectrum of bound states with $k = i|k|$ ($k^2 = mE_2/\hbar^2$) corresponds to the solutions of the equa-

tion

$$1 + gk \frac{m}{\hbar^2} \frac{i\pi}{4} \int_0^\infty dr r \phi(k, r) V(r) H_1^{(1)}(kr) = 0, \quad (\text{A1})$$

where $H_1^{(1)}$ is the first Hankel function of order one [40]. We focus on the ground state in the weak binding limit, $k \rightarrow 0$, and write eq. (A1) in the form

$$1 + kg \frac{m}{\hbar^2} \frac{i\pi}{4} \int_0^\infty dr r \phi(0, r) V(r) \left(\frac{i}{\pi} kr (\ln(kr/2) + \gamma - 1/2 - i\pi/2) - \frac{2i}{\pi kr} \right) + o(k^2 \ln kR_0) = 0, \quad (\text{A2})$$

where $\gamma = 0.577\dots$ is the Euler-Mascheroni constant and where we use the regular zero energy solution from Eq. (2). Eq. (A2) with $k = 0$ defines g_2^{cr} as the smallest solution of the equation:

$$1 + g_2^{cr} \frac{m}{2\hbar^2} \int_0^\infty dr \phi(r) V(r) = 0, \quad (\text{A3})$$

which from Eq. (3) is seen to correspond to the solution of infinite scattering length, $a \rightarrow \infty$. If g is slightly larger than g_2^{cr} then the ground state is bound and the binding energy satisfies the equation

$$AE_2 \ln(|E_2|B) + g_2^{cr} - g \simeq 0, \quad (\text{A4})$$

where (A, B, g_2^{cr}) are positive constants. This dependency was used to extract an accurate value of g_2^{cr} by fitting the numerically calculated E_2 as function of g .

Appendix B: Three-body problem in the hyperspherical formalism

Here we present the derivations that lead to the Eqs.(12) and (13). We show the approach to solve Eq.(9) with the wave function in Eq.(10). The set $\phi_{Mm_x}(\rho, \alpha)$, where for simplicity we use $i = 1$ and omit the related index, solves the following system of integro-differential equations [5]

$$\begin{aligned} & \left(-\frac{\partial^2}{\partial \alpha^2} - 2 \cot(2\alpha) \frac{\partial}{\partial \alpha} + \frac{m_x^2}{\sin^2 \alpha} + \frac{m_y^2}{\cos^2 \alpha} - \lambda_M \right) \phi_{Mm_x} \\ &= -g \frac{2m\rho^2}{\hbar^2} V(\sqrt{2}\rho \sin \alpha) \left(\phi_{Mm_x} + \sum_{m'_x} R_{Mm_x m'_x} \right), \end{aligned} \quad (\text{B1})$$

where $m_y = M - m_x$ and the coupling term $R_{Mm_x m'_x}$ is defined as

$$\begin{aligned} R_{Mm_x m'_x} &= \frac{1}{4\pi^2} \sum_{j \neq 1} \int d\Theta_x d\Theta_y e^{im_x \Theta_x} e^{i(M-m_x)\Theta_y} \\ &\times \phi_{Mm'_x}(\rho, \alpha_j) e^{-im'_x \Theta_{xj}} e^{-i(M-m'_x)\Theta_{yj}}. \end{aligned} \quad (\text{B2})$$

Non-interacting case. Let us first consider the situation when $V = 0$, which also defines the extreme short-distance behavior of λ_M for potentials diverging slower than $1/r^2$ at zero. In this situation the system of equations (B1) decouples

$$\left(-\frac{\partial^2}{\partial \alpha^2} - 2 \cot(2\alpha) \frac{\partial}{\partial \alpha} + \frac{m_x^2}{\sin^2 \alpha} + \frac{m_y^2}{\cos^2 \alpha} - \lambda_M \right) \phi_{Mm_x}^{(0)} = 0, \quad (\text{B3})$$

where the superscript 0 tells us that we work with free particles. The solutions that are regular at $\alpha = 0, \pi/2$ are [5],

$$\phi_{Mm_x}^{(0)} = N_{Mm_x}^{(0)} \sin^{|m_x|}(\alpha) \cos^{|m_y|}(\alpha) P_n^{(|m_x|, |m_y|)}(\cos(2\alpha)), \quad (\text{B4})$$

where $P_n^{(|m_x|, |m_y|)}$ is the Jacobi polynomial [40], $N_{Mm_x}^{(0)}$ is the normalization constant, and n is a non-negative integer related to the eigenvalue λ_M by $\lambda_M = K(K+2)$, $K = 2n + |m_x| + |M - m_x|$. This result can also be used to determine the behavior of λ_M near $\rho = 0$, since the right-hand side of Eq.(B1) contains the factor ρ^2 . From this we learn that for $M = 1$ the lowest centrifugal barrier is determined by $m_x = 1$, $n = 1$, $K = 3$ (since the antisymmetric wave function with $m_x = 1$ and $n = 0$ is zero). For $M = 0$ the lowest barrier arises from $m_x = 1$, $n = 0$, $K = 2$.

Interacting case. We aim to find the large-distance behavior of λ_M . We introduce an angle $\alpha_0 = R_0/(\sqrt{2}\rho) \rightarrow 0$, such that for $\alpha > \alpha_0$ Eq.(B1) is the non-interacting case (right-hand side is zero) with the regular boundary condition at $\alpha = \pi/2$ and solved by

$$\begin{aligned} \phi_{Mm_x}(\rho, \alpha) &= N_{Mm_x}(\rho) \sin^{|m_x|}(\alpha) \cos^{|M-m_x|}(\alpha) \\ &\times P_{\nu_{Mm_x}}^{(|M-m_x|, |m_x|)}(-\cos(2\alpha)), \end{aligned} \quad (\text{B5})$$

where $\nu_{Mm_x}(\rho)$ is given by $\lambda_M(\rho) = (2\nu_{Mm_x}(\rho) + |m_x| + |M - m_x|)(2\nu_{Mm_x}(\rho) + |m_x| + |M - m_x| + 2)$. This wave function diverges for $\alpha \rightarrow 0$, where the interacting solution has to be used. To obtain the solution we use that only the components with $|m_x| = 1$ are necessary to lowest order, since higher partial waves are suppressed at small interparticle distances, i.e. $\alpha < \alpha_0$, equivalent to large distances. More precisely, in the absence of additional resonances in the higher partial wave channels with $|m_x| > 1$ one can show that $\nu_{Mm_x}(\rho) = n + O((b/\rho)^{2|m_x|})$ where n is an integer (corresponding to a free solution) [5]. Such terms will therefore vanish much faster than the $|m_x| = 1$ terms and can thus be neglected.

Case with $M = 1$. For $M = 1$ we need to solve the following system of equations for small α

$$\begin{aligned} & \left(-\frac{\partial^2}{\partial \alpha^2} - 2 \cot(2\alpha) \frac{\partial}{\partial \alpha} + \frac{1}{\sin^2 \alpha} - \lambda_1(\rho) \right) \phi_{11}(\alpha, \rho) = \\ & -\frac{2g m \rho^2}{\hbar^2} V(\sqrt{2}\rho \alpha) (\phi_{11}(\alpha, \rho) + R_{111} + R_{11-1}), \end{aligned} \quad (\text{B6})$$

$$\left(-\frac{\partial^2}{\partial \alpha^2} - 2 \cot(2\alpha) \frac{\partial}{\partial \alpha} + \frac{1}{\sin^2 \alpha} + \frac{4}{\cos^2 \alpha} - \lambda_1 \right) \phi_{1-1} = -\frac{2gm\rho^2}{\hbar^2} V(\sqrt{2}\rho\alpha)(\phi_{1-1} + R_{1-11} + R_{1-1-1}). \quad (\text{B7})$$

We note that $\nu_{1-1} = \nu_{11} - 1$, since they should yield the same λ_1 , i.e. $(2\nu_{11} + 1)(2\nu_{11} + 3) = (2\nu_{1-1} +$

$3)(2\nu_{1-1} + 5)$. For simplicity from now on we will write $\nu_{11} = \nu$. Now we expand the wave functions $\phi_{Mm'_x}(\rho, \alpha_j) e^{-im'_x \Theta_{xj}} e^{-i(M-m'_x)\Theta_{yj}}$ with $j = 2, 3$ in the vicinity of $\alpha = 0$ which leads to the coupling terms

$$\begin{aligned} R_{111} &\simeq \alpha r_{11} N_{11}; & r_{11} &= -{}_2F_1(-\nu, \nu + 2, 1, 1/4) - \frac{3\nu(\nu + 2)}{4} {}_2F_1(-\nu + 1, \nu + 3, 2, 1/4); \\ R_{11-1} &\simeq \alpha r_{1-1} N_{1-1}; & r_{1-1} &= \frac{\Gamma(\nu + 2)}{\Gamma(\nu)} \left(\frac{3}{4} {}_2F_1(-\nu + 1, \nu + 3, 3, 1/4) - \frac{(\nu - 1)(\nu + 3)}{32} {}_2F_1(-\nu + 2, \nu + 4, 4, 1/4) \right); \\ R_{1-1-1} &\simeq \alpha r_{-1-1} N_{1-1}; & r_{-1-1} &= \frac{\Gamma(\nu + 2)}{\Gamma(\nu)} \left(-\frac{{}_2F_1(-\nu + 1, \nu + 3, 3, 1/4)}{8} - \frac{(\nu - 1)(\nu + 3)}{32} {}_2F_1(-\nu + 2, \nu + 4, 4, 1/4) \right); \\ R_{1-11} &\simeq \alpha r_{-11} N_{11}; & r_{-11} &= -\frac{3\nu(\nu + 2)}{4} {}_2F_1(-\nu + 1, \nu + 3, 2, 1/4); \end{aligned} \quad (\text{B8})$$

where $\Gamma(x)$ is the gamma function and ${}_2F_1$ is the ordinary hypergeometric function [40] where all couplings $R \sim \alpha$ as for $|m_x| = 1$.

The homogeneous part of Eqs.(B6) and (B7) for small α has the main contribution from the two-dimensional two-body equation, Eq.(1), as seen by using the substitution $r = \sqrt{2}\rho\alpha$. One solution to the inhomogeneous part is $\phi_{11} = -(R_{11} + R_{1-1})$ and $\phi_{1-1} = -(R_{-11} + R_{-1-1})$. In this way we find the solutions for $\alpha < \alpha_0$

$$\phi_{11} = C \left(\rho\alpha - \frac{a^2}{2\rho\alpha} \right) - N_{11}\alpha r_{11} - N_{1-1}\alpha r_{1-1}, \quad (\text{B9})$$

$$\phi_{1-1} = C_1 \left(\rho\alpha - \frac{a^2}{2\rho\alpha} \right) - N_{11}\alpha r_{-11} - N_{1-1}\alpha r_{-1-1}, \quad (\text{B10})$$

where $C(\rho), C_1(\rho), N_{11}(\rho)$ and $N_{1-1}(\rho)$ are functions that up to normalization should be determined by matching the solutions and their first derivatives for $\alpha > \alpha_0$ and $\alpha < \alpha_0$ at α_0 . This matching can be done only for specific values, λ_1 , that can be obtained from the following equation

$$\frac{\left(P_\nu^{(0,1)}(-\cos(2\alpha_0)) + \frac{\alpha_0}{2} \frac{\partial P_\nu^{(0,1)}(-\cos(2\alpha_0))}{\partial \alpha} + r_{11} \right) \times \left(P_{\nu-1}^{(2,1)}(-\cos(2\alpha_0)) + \frac{\alpha_0}{2} \frac{\partial P_{\nu-1}^{(2,1)}(-\cos(2\alpha_0))}{\partial \alpha} + r_{-1-1} \right)}{r_{-11}r_{1-1}} = 1, \quad (\text{B11})$$

where we took the limit $a \rightarrow \infty$, since it defines the two-body threshold for binding. To simplify this equation we

use the following identities, see for example Ref. [5],

$$P_\nu^{(a,b)}(-x) = \cos(\pi\nu) P_\nu^{(b,a)}(x) - \sin(\pi\nu) Q_\nu^{(b,a)}(x), \quad (\text{B12})$$

$$Q_\nu^{(1,0)}(\cos(2\alpha)) \simeq \frac{\Gamma(\nu + 2)}{\pi\Gamma(\nu + 1)} \left[-2\gamma + 1 - \psi_\Gamma(1 + \nu) - \psi_\Gamma(\nu + 2) - 2 \ln(\alpha) \right] + \frac{\Gamma(\nu + 1)}{\pi\Gamma(\nu + 2)} \frac{1}{\alpha^2}, \quad (\text{B13})$$

$$Q_{\nu-1}^{(1,2)}(\cos(2\alpha)) \simeq \frac{\Gamma(\nu + 1)}{\pi\Gamma(\nu)} \left[-2\gamma + 1 - \psi_\Gamma(\nu) - \psi_\Gamma(\nu + 2) - 2 \ln(\alpha) \right] + \frac{\Gamma(\nu + 2)}{\pi\Gamma(\nu + 3)} \frac{1}{\alpha^2}, \quad (\text{B14})$$

where ψ_Γ is the digamma function. These identities allow Eq.(B11) to be rewritten

$$\frac{\left(\frac{\Gamma(\nu + 2)}{\Gamma(\nu + 1)} \left(\cos(\pi\nu) + \frac{\sin(\pi\nu)}{\pi} [\psi_\Gamma(1 + \nu) + 2 \ln \alpha_0] \right) + r_{11} \right) \times \left(\frac{\Gamma(\nu + 1)}{\Gamma(\nu)} \left(\cos(\pi\nu) + \frac{\sin(\pi\nu)}{\pi} [\psi_\Gamma(\nu) + 2 \ln \alpha_0] \right) + r_{-1-1} \right)}{r_{-11}r_{1-1}} = -1,$$

where we neglect terms smaller than $|\ln \alpha_0|$ in the limit of $\alpha_0 \rightarrow 0$. The smallest solution to this equation is $\nu = -1 + \delta\nu$, with $(\delta\nu)^2 = -\frac{4}{9(\ln \alpha_0)^2}$. This solution yields $\lambda_1 = (2\nu + 1)(2\nu + 3) = -1 - 16/(9(\ln \alpha_0)^2)$, where $\alpha_0 \sim 1/\rho$. As we discuss in the main part of the paper this solution produces the infinite tower of states with the double exponential scaling.

Validity of the derived large-distance behavior of λ_1 at $1/a = 0$. Before applying this adiabatic potential we

need to discuss its validity. To do so we first need to estimate what will be changed by adding higher order terms in Eqs.(B9) and (B10); and second we need to calculate the lowest order coupling term [5],

$$Q = \langle \Phi_1 | \frac{\partial^2}{\partial \rho^2} | \Phi_1 \rangle_\Omega, \quad (\text{B15})$$

where the averaging over all angles is taken for normalized angular wave functions, $\langle \Phi_1 | \Phi_1 \rangle_\Omega = 1$. First, the higher order large-distance effects on the angular wave functions are necessary, since their neglect is the only assumption made after we decided to use only partial waves with $|m_x| = 1$. Second, inclusion of the diagonal coupling yields an upper bound for the exact binding energy, which together with the lower bound produced by λ_1 establishes bounds for the exact three-body binding energy. It was very recently shown [18] that the higher order terms ($\sim 1/\rho^2$) in the solution to the homogeneous angular part of Eqs.(B6) and (B7) contribute as

$$Q = C(\rho) \int_0^{\alpha_0} u(\sqrt{2}\alpha\rho) \frac{\partial^2}{\partial \rho^2} C(\rho) u(\sqrt{2}\alpha\rho) \sin(2\alpha) d\alpha \\ + N_{11}(\rho) \int_{\alpha_0}^{\pi/2} \sin(\alpha) P_\nu^{(0,1)}(-\cos(2\alpha)) \frac{\partial^2}{\partial \rho^2} N_{11}(\rho) \sin(\alpha) P_\nu^{(0,1)}(-\cos(2\alpha)) \sin(2\alpha) d\alpha, \quad (\text{B17})$$

where $u(x)$ is the two-body wave function decreasing as $1/x$ at infinity, the constants $C(\rho) = -\frac{\rho}{\sqrt{\ln(\rho)}}$ and $N_{11}(\rho) = \frac{1}{\sqrt{2 \ln(\rho)}}$ are determined to satisfy normalization and boundary conditions at $\alpha = \alpha_0$. After straightforward but tedious calculation we obtain $Q = -Y/(\rho^2 \ln(\rho/R_0))$. We know [5] that Q is negative, and consequently Y must be positive. This can also easily be confirmed directly by rewriting Y as

$$Y = \frac{\int_0^\infty x \left[\frac{\partial u(x)x}{\partial x} \right]^2 dx}{\lim_{x \rightarrow \infty} (xu(x))^2}. \quad (\text{B18})$$

This means that the derived adiabatic potential necessarily should be supplemented with both the Q term

$-Y/\ln(\rho/R_0)$ to $\lambda_1(\rho)$, where

$$Y = -1 - \frac{\int_0^\infty dx x^3 V(x) u(x)^2}{\lim_{x \rightarrow \infty} (xu(x))^2}. \quad (\text{B16})$$

This surprising effect can be understood since the boundary conditions require that the constants in Eqs.(B9) and (B10) must satisfy $C(\rho) \sim \rho N_{11}(\rho)$. This means that a higher order term in Eqs.(B6) and (B7) may be of the same order as the couplings neglected in Eqs.(B9) and (B10). In Ref. [18] it was pointed out that such an effect means that two-body observables alone is not sufficient to reproduce the correct asymptotic large-distance structure of λ_1 . Thus, universal behavior is not guaranteed.

To obtain an upper bound we estimate the diagonal coupling term, Q , from Eq.(B15) as in Ref. [5]. For large ρ we find up to terms of order $\sim \left(\frac{1}{\rho^2 \ln^2(\rho/R_0)} \right)$ the explicit expression:

and the term, $-Y/(\rho^2 \ln(\rho/R_0))$, obtained by inclusion of next-to-leading order terms in the solution to the homogeneous part of Eqs.(B6) and (B7). It turns out that the leading contribution in the Q term cancels exactly the $-Y/(\rho^2 \ln(\rho/R_0))$ term. Thus, to make a rigorous conclusion about the allowed interval for the three-body binding energy, the next-to-leading order in Q term should be calculated. This investigation is, however, out of scope of the present paper but it should be the focus in future more detailed and more elaborate work.

Case with $M = 0$. This case is not very different from the $M = 1$ just discussed above. We therefore only give the resulting λ_0 , and the couplings that are needed to solve the corresponding equations. The couplings for $\alpha \rightarrow 0$ take the form

$$R_{011} \simeq \alpha r_{11} N_{01}; r_{11} = \frac{\Gamma(\nu+2)}{\Gamma(\nu+1)} \left(\frac{1}{2} {}_2F_1(-\nu, \nu+3, 2, 1/4) + \frac{3\nu(\nu+3)}{16} {}_2F_1(-\nu+1, \nu+4, 3, 1/4) \right);$$

$$\begin{aligned}
R_{01-1} &\simeq \alpha r_{1-1} N_{0-1}; r_{1-1} = \frac{\Gamma(\nu+2)}{\Gamma(\nu+1)} \left(-\frac{3}{2} {}_2F_1(-\nu, \nu+3, 2, 1/4) + \frac{3\nu(\nu+3)}{16} {}_2F_1(-\nu+1, \nu+4, 3, 1/4) \right); \\
R_{0-11} &\simeq \alpha r_{-11} N_{01}; r_{-11} = \frac{\Gamma(\nu+2)}{\Gamma(\nu+1)} \left(-\frac{3}{2} {}_2F_1(-\nu, \nu+3, 2, 1/4) + \frac{3\nu(\nu+3)}{16} {}_2F_1(-\nu+1, \nu+4, 3, 1/4) \right); \\
R_{0-1-1} &\simeq \alpha r_{-1-1} N_{0-1}; r_{-1-1} = \frac{\Gamma(\nu+2)}{\Gamma(\nu+1)} \left(\frac{1}{2} {}_2F_1(-\nu, \nu+3, 2, 1/4) + \frac{3\nu(\nu+3)}{16} {}_2F_1(-\nu+1, \nu+4, 3, 1/4) \right); \quad (\text{B19})
\end{aligned}$$

where ν defines λ_0 as $\lambda_0 = (2\nu+2)(2\nu+4)$. In the same way as we obtained Eq. (B11) we derive the following equation for ν

$$\left(P_\nu^{(1,1)}(-\cos(2\alpha_0)) + \frac{\alpha_0}{2} \frac{\partial P_\nu^{(1,1)}(-\cos(2\alpha_0))}{\partial \alpha} + r_{11} \right)^2 = r_{11}^2 \quad (\text{B20})$$

This equation has a particular solution $\nu = -1 + \frac{4}{3 \ln \alpha_0}$, which produces $\lambda_0 = \frac{16}{3 \ln \alpha_0}$. The corresponding adia-

batic potential was presented in the main part of this paper. We also note that to determine the large-distance behavior up to terms proportional to $1/\ln(\rho/R_0)$ we need an investigation similar to the one provided for $M = 1$. However, since the leading term in the adiabatic potential, $3/(4\rho^2)$, only marginally allows universal weakly-bound states the results of such calculations are not expected to be particularly interesting. In the $M = 0$ channel the most important physics comes from the non-universal adiabatic potential at short-distance.

-
- [1] V. Efimov, *Yad. Fiz* **12**, 1080 (1970); *Sov. J. Nucl. Phys.* **12**, 589 (1971).
- [2] M. V. Zhukov *et al.*, *Physics Reports* **231**, 151 (1993).
- [3] J.-M. Richard and S. Fleck, *Phys. Rev. Lett.* **73**, 1464 (1994).
- [4] S. Moszkowski *et al.*, *Phys. Rev. A* **62**, 032504 (2000).
- [5] E. Nielsen, D. V. Fedorov, A. S. Jensen, and E. Garrido, *Physics Reports* **347**, 373 (2001).
- [6] A. S. Jensen, K. Riisager, D. V. Fedorov, and E. Garrido, *Rev. Mod. Phys.* **76**, 215 (2004).
- [7] E. Braaten and H. W. Hammer, *Phys. Rep.* **428**, 259 (2006).
- [8] N. A. Baas *et al.*, *Physics of Atomic Nuclei*, **77**, 361 (2014).
- [9] J. H. Macek and J. Sternberg, *Phys. Rev. Lett.* **97**, 023201 (2006).
- [10] N. T. Zinner and A. S. Jensen, *J. Phys. G: Nucl. Part. Phys.* **40**, 053101 (2013).
- [11] E. Nielsen, D. V. Fedorov, and A. S. Jensen, *Phys. Rev. A* **56**, 3287 (1997).
- [12] A. G. Volosniev, D. V. Fedorov, A. S. Jensen, and N. T. Zinner, *Eur. Phys. J. D* **67**, 95 (2013).
- [13] E. Nielsen, D. V. Fedorov, and A. S. Jensen, *Few Body Syst.* **27**, 15 (1999).
- [14] L. W. Bruch and J. A. Tjon, *Phys. Rev. A* **19**, 425 (1979).
- [15] S. A. Vugal'ter and G. M. Zhislin, *Theor. Math. Phys.* **55**, 493 (1983).
- [16] Y. Nishida, S. Moroz, and D. T. Son, *Phys. Rev. Lett.* **110**, 235301 (2013).
- [17] J. Levinsen, N. R. Cooper, and V. Gurarie, *Phys. Rev. A* **78**, 063616 (2008).
- [18] C. Gao and Z. Yu, arXiv:1401.0965 (2014)
- [19] I. Bloch, J. Dalibard, and W. Zwerger, *Rev. Mod. Phys.* **80**, 885 (2008).
- [20] S. Giorgini, L. P. Pitaevskii, and S. Stringari, *Rev. Mod. Phys.* **80**, 1225 (2008).
- [21] L. Pricoupenko, *Phys. Rev. Lett.* **100**, 170404 (2008).
- [22] R. G. Newton, *Math. Phys.* **27**, 2720 (1986).
- [23] A. G. Volosniev: *Few-Body Systems in Low-Dimensional Geometries*, (PhD thesis, Aarhus University, 2013).
- [24] Y. Suzuki and K. Varga: *Stochastic Variational Approach to Quantum-Mechanical Few-Body Problems* (Springer, Berlin, 1998).
- [25] J. Mitroy *et al.*, *Rev. Mod. Phys.* **85**, 693 (2013).
- [26] A. G. Volosniev, D. V. Fedorov, A. S. Jensen, and N. T. Zinner, *Phys. Rev. Lett.* **106**, 250401 (2011).
- [27] D. V. Fedorov and A. S. Jensen, *Phys. Rev. Lett.* **71**, 4103 (1993).
- [28] A. S. Jensen, E. Garrido, and D. V. Fedorov, *Few-Body Syst.* **22**, 193 (1997).
- [29] H. T. Coelho and J. E. Hornos, *Phys. Rev. A* **43**, 6379 (1991).
- [30] K. Chadan, N. N. Khuri, A. Martin, and T. T. Wu, *J. Math. Phys.* **44**, 406 (2003).
- [31] T. Kraemer *et al.*, *Nature* **440**, 315 (2006).
- [32] S. E. Pollack, D. Dries, and R. G. Hulet, *Science* **326**, 1683 (2009).
- [33] M. Zaccanti *et al.*, *Nature Phys.* **5**, 586 (2009).
- [34] N. Gross, Z. Shotan, S. Kokoelmans, and L. Khaykovich, *Phys. Rev. Lett.* **103**, 163202 (2009).
- [35] T. Lompe, T. B. Ottenstein, F. Serwane, A. N. Wenz, G. Zürn, and S. Jochim, *Science* **330**, 940 (2010).
- [36] S. Nakajima, M. Horikoshi, T. Mukaiyama, P. Naidon, and M. Ueda, *Phys. Rev. Lett.* **106**, 143201 (2011).
- [37] O. Machtey, Z. Shotan, N. Gross, and L. Khaykovich, *Phys. Rev. Lett.* **108**, 210406 (2012).
- [38] C. Chin, R. Grimm, P. S. Julienne, and E. Tiesinga, *Rev. Mod. Phys.* **82**, 1225 (2010).
- [39] W. G. Gibson, *Physics Letters A* **117**, 107 (1986).
- [40] M. Abramowitz and I. Stegun: *Handbook of Mathematical Functions with Formulas, Graphs, and Mathematical Tables* (Dover, New York, 1964).